Effect of fluid flow on the fluctuations at the surface of an elastic medium

V. Kumaran
Department of Chemical Engineering, Indian Institute of Science, Bangalore 560 012, India

(Received 8 August 1994; accepted 15 November 1994)

The effect of a linear shear flow of a Newtonian fluid in the region $0<z<\infty$ on the fluctuations at the surface of an elastic medium of thickness H in the region $-H<z<0$ is analyzed in the regime $\mathrm{Re}\gg 1$ and $\Lambda\sim 1$, where $\mathrm{Re}=\rho\gamma H^2/\eta$ is the Reynolds number and $\Lambda=(\rho\gamma^2 H^2/E)^{1/2}$ is the ratio of the inertial stresses in the fluid and the elastic stresses in the solid. Here ρ and η are the fluid density and viscosity, E is the coefficient of elasticity of the solid, and γ is the mean strain rate in the fluid. A linear analysis is used to determine the effect of the flow on the fluctuations in the surface displacement, and an asymptotic expansion in the small parameter $\epsilon=(\Lambda/\mathrm{Re})$ is employed. The dynamics in the bulk of the fluid is inviscid in the leading approximation, and the leading order growth rate is imaginary because energy is conserved in the absence of viscous dissipation. There are multiple frequencies of oscillation, all of which satisfy the equations of motion. An increase in the fluid velocity increases the frequency of the downstream traveling waves, and decreases the frequency of the upstream traveling waves. The structure factor for the surface modes of the upstream traveling waves increases with an increase in the fluid velocity because the kinetic energy of the fluctuations decreases due to the lower frequency. An opposite effect is observed for the downstream traveling waves; in addition, it is observed that the structure factor has a double-peaked structure and reaches zero at an intermediate value at sufficiently high velocities. This is due to a divergence in the ratio of the tangential and normal displacements, and a consequent divergence in the energy required for the normal fluctuations at the surface. There is an $O(\epsilon^{1/2})$ correction to the growth rate due to the presence of a viscous boundary layer of thickness $H\epsilon^{1/2}$ in the fluid at the interface. The $O(\epsilon^{1/2})$ calculation shows that the real part of the growth rate is negative for all values of Λ and wave number k, except along certain lines in the $\Lambda-k$ parameter space where the real part of the growth rate is zero, because the amplitude of the boundary layer velocity becomes zero along these lines. The real part of the $O(\epsilon)$ correction to the growth rate at these points is negative, indicating the presence of a small stabilizing effect due to the dissipation in the bulk of the fluid and the elastic medium.

I. INTRODUCTION

The flow of a fluid near an elastic surface is of interest in practical applications such as biological systems, where the transport of fluid takes place through vessels with flexible walls, biochemical and pharmaceutical industries where many processes involve the transport and diffusion of fluids through gels and membranes, and in other industrial applications such as polymer tribology where surface oscillations provide a mechanism for energy dissipation. The surface fluctuations in polymer gels in contact with air has been previously studied.[1,2] However, it has recently been realized both theoretically[3] and experimentally[4–7] that flow of a fluid at the surface could significantly affect the dynamics of the interface. Here, the effect of a high Reynolds number shear flow on the fluctuations at the surface of an elastic medium is examined. It is shown that some of the characteristics of the surface fluctuations could be significantly altered by the fluid flow.

The majority of previous analyses have used a single fluid model, where the polymer is treated as a viscoelastic fluid, and is described by the non-Newtonian Navier–Stokes equations where the stress is a nonlinear function of the strain rate. A two-fluid model was used by Harden, Pleiner, and Pincus[1] to determine the surface modes on a semi-infinite gel. In the two-fluid model, coupled equations are written for the fluid velocity and the displacement field in the polymer network. These equations are solved in the ''infinite coupling limit,'' where the coupling constant between the network and the fluid is large, so their velocities are assumed to be equal in the leading order approximation. In addition to the viscous shear stress due to the fluid flow, there is an additional elastic stress due to the polymer network which gives rise to features not observed in classical fluids.

The fluctuations at the surface of a polymer gel of finite thickness was analyzed using a two-fluid model by the author[2] in the limit where the elastic oscillation time for the strain field in the polymer is small compared to the viscous relaxation time. The smallness of the viscous effects permits an asymptotic analysis, where the viscous terms are neglected at leading order, and there is a balance between the inertial and the elastic stresses. The leading order decay rate of fluctuations is purely imaginary since energy is conserved in the leading approximation. There are multiple frequencies of oscillation, all of which are consistent with the equations of motion. The structure factor for the height correlations is determined from the total energy of the fluctuations, which is the sum of the kinetic energy of motion and the elastic strain energy. An interesting finding is that the frequency and structure factor depend not only the boundary conditions at the free surface, but also on the conditions at the other surface.

The study of the flow near a flexible wall has been mo-

 0021-9606/95/102(8)/3452/9/$6.00

tivated by marine and aerodynamics applications. There have been many theoretical analyses of the modification of the flow near an elastic surface (for a recent review, see Riley *et al.*[8]). Here, the dynamics of the surface is approximated by a lumped parameter model, and the equation for the surface contains an inertial term proportional to the normal acceleration of the surface, a spring term proportional to the normal displacement, a damping term proportional to the normal velocity and possibly surface tension and curvature terms. The effect of flexibility of the surface on the hydrodynamic stability has been studied by Benjamin[9,10] and Landahl.[11] They found that a flexible surface tends to delay the onset of the Tollmien–Schlichting instability, which is the destabilizing mechanism in flow past rigid surfaces. In addition, there is an additional mode of instability, called the flow induced surface instability, which is not present in the flow past a rigid surface. Recently, there has been numerical work done on the flow past compliant surfaces[12,13] where a numerical solution of the Orr–Sommerfeld equation is obtained. These studies focus on the effect of surface flexibility on the stability of the flow, and so they do not account for the dynamics of the elastic surface in an exact fashion.

The effect of a viscous flow (zero Reynolds number) on the surface fluctuations of a polymer gel was studied by Kumaran, Fredrickson, and Pincus.[3] This showed that even in the absence of fluid inertia, there is an instability when the strain rate in the fluid exceeds a critical value. This instability is driven by the transport of energy from the mean flow to the fluctuations due to the deformation work done by the mean flow at the elastic surface. The critical velocity for the onset of an instability has a complex dependence on the ratio of the fluid and gel thicknesses, and the ratio of viscosities of the fluid and the gel.

There have been some experimental studies of fluid flow past an elastic surface. Hansen and Hunston[4] observed that when a plasticol coated disk is spun in a Newtonian fluid, there is an increase in the drag force when the Reynolds number is increased beyond a critical value, and a traveling wave pattern appears on the disk at the onset of instability. Silberberg[5] reported that the critical Reynolds number in the Hansen and Hunston[4] experiments was proportional to $R_G^{1/2}$, where R_G is a dimensionless number $(Ea^3\rho/4H\eta^2)$, E is the modulus of elasticity of the surface, ρ is the fluid density, H is the thickness, a is the radius of the disk, and η is the fluid viscosity. In addition, Krindel and Silberberg[6] studied the flow of a fluid through a tube with gel walls, and they observed an increased drag force for $\mathrm{Re}>R_G$, where $R_G=(ER^3\rho/4H\eta)$, R is the radius of the tube, and H is the thickness of the wall in this case. The low Reynolds number analysis of Kumaran *et al.*[3] correctly predicted that the critical Reynolds number is proportional to R_G, though they had a different prefactor because they considered a flow in a two dimensional channel instead of a tube.

In the present analysis, we consider the linear flow of a fluid of infinite thickness adjacent to a elastic surface of thickness H. The Reynolds number, $\mathrm{Re}=(\rho\gamma H^2/\eta)$, is large, while the parameter $\Lambda=(\rho\gamma^2H^2/E)^{1/2}$ is $O(1)$. Here, γ is the strain rate in the fluid, ρ and η are the fluid density and viscosity, and E is the elasticity of the surface. The parameter

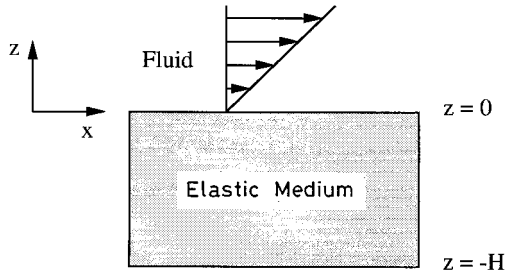

FIG. 1. Fluid and gel configuration and the coordinate system.

Λ is the ratio of the inertial stresses in the fluid and the elastic stresses in the surface, and the condition $\Lambda=O(1)$ is necessary for the surface dynamics to significantly influence the fluid flow. The model for the fluid and solid dynamics is given in Sec. II, and the dynamics of the fluctuations at the surface is determined using a linear analysis in Sec. III. An asymptotic analysis in the small parameter $\epsilon=(\Lambda/\mathrm{Re})$ is used, and the fluid viscosity is neglected in the leading approximation. We find that the leading order growth rate of the fluctuations is always imaginary, and the fluctuations are neutrally stable in the leading approximation because there is no viscous dissipation. The decay rate of the fluctuations, which is due to the dissipation in the viscous boundary layer, is $O(\epsilon^{1/2})$ smaller than the leading order frequency.

The characteristics of the leading order frequency and structure factor are similar to that for the surface modes at the surface of a gel in contact with air,[2] though the flow does have a significant effect on the structure factor. However, the decay rate of the fluctuations is qualitatively different for the present case, because the leading order dissipation of energy takes place in a viscous boundary layer at the interface and not in the bulk of the fluid or the elastic medium. The important results are summarized in Sec. IV, and the experimental results of Hansen and Hunston[4] are compared with the predictions of the analysis.

II. MODEL

The system consists of an incompressible elastic medium of thickness H, modulus of elasticity E, viscosity η_g, and infinite lateral extent which is fixed to a rigid surface at $z=-H$ as shown in Fig. 1. There is a Newtonian fluid of viscosity η and density ρ in the region $0<z<\infty$, and the fluid is flowing with a constant strain rate γ in the x direction

$$\bar{v}=\gamma z. \tag{1}$$

As mentioned in the Introduction, we consider a flow where the Reynolds number, $\mathrm{Re}=(\rho\gamma H^2/\eta)$, is large, while the parameter $\Lambda=(\rho\gamma^2H^2/E)^{1/2}$, is $O(1)$. The parameter Λ is the ratio of the inertial forces in the fluid and the elastic forces in the medium, and the elastic stresses in the medium are comparable to the inertial stresses in the fluid for $\Lambda\sim O(1)$. In this limit, it is appropriate to nondimensionalize the lengths in the equations of motion by H, the time by $(\rho H^2/E)^{1/2}$, and the velocities by $(E/\rho)^{1/2}$. The nondimensional mean velocity (1) is

$$\bar{v}=\Lambda z. \tag{2}$$

The equations for the fluid velocity field v_i are the Navier–Stokes mass and momentum equations

$$\partial_i v_i=0, \tag{3}$$

$$\partial_t v_i+v_j\partial_j v_i=-\partial_i p+\epsilon\partial_j^2 v_i. \tag{4}$$

Here, $\partial_t=(\partial/\partial t)$, $\partial_i=(\partial/\partial x_i)$, and $\epsilon=(\Lambda/\mathrm{Re})$ is the small parameter that will be used for the asymptotic expansion. The stresses in the fluid are scaled by the shear modulus, E, as before

$$\tau_{zz}=-p+2\epsilon\partial_z v_z, \tag{5}$$

$$\tau_{xz}=\epsilon(\partial_z v_x+\partial_x v_z). \tag{6}$$

The dynamics of the elastic medium is described using a displacement field u_i, which represents the displacement of the material points in the solid from their equilibrium positions due to the stresses acting at the surface. The conservation equations for the displacement field used here are similar to those used for polymer gels[1,2]

$$\partial_i u_i=0, \tag{7}$$

$$\partial_t^2 u_i=-\partial_i p+\partial_j^2 u_i+\epsilon\eta'\partial_j^2(\partial_t u_i). \tag{8}$$

Here the pressure, p, is nondimensionalized by the shear modulus, E, and $\eta'=(\eta_g/\eta)$ is the ratio of the solid and fluid viscosities. Equation (7) is the mass conservation equation for an incompressible elastic medium, while (8) is the momentum balance equation. In the latter, the term on the left side is the rate of change of momentum in a volume element of the elastic medium, while the terms on the right represent the divergence of the pressure, the divergence of the elastic stress due to the strain in the medium,[14] and the divergence of the viscous stress due to the strain rate, respectively. The shear and normal stresses in the elastic solid, nondimensionalized by the shear modulus E, are

$$\sigma_{zz}=-p+2[1+\epsilon\eta'\partial_t](\partial_z u_z), \tag{9}$$

$$\sigma_{xz}=[1+\epsilon\eta'\partial_t](\partial_z u_x+\partial_x u_z). \tag{10}$$

The boundary conditions for the elastic medium at the surface $z=-H$ are the zero displacement conditions

$$u_z=0, \quad u_x=0, \tag{11}$$

while the appropriate boundary conditions at the interface between the fluid and the elastic medium are the continuity of velocity and stress

$$\begin{aligned} &v_z=\partial_t u_z, \quad v_x=\partial_t u_x,\\ &\tau_{zz}=\sigma_{zz}, \quad \tau_{xz}=\sigma_{xz}. \end{aligned} \tag{12}$$

Equations (3), (4), (7), and (8), along with the boundary conditions at $z=-H$, Eq. (11), and the boundary conditions at the interface (12) can be solved to determine the growth rate of fluctuations.

III. ANALYSIS

In this section, an asymptotic analysis in the small parameter ϵ is used to determine the growth rate of the surface fluctuations. Small perturbations are placed on the displacement and velocity fields of the form

$$\begin{aligned} u_i&=(2\pi)^{-1}\int dk\ \tilde{u}_i(z)\exp(ikx+\alpha t),\\ v_i&=(2\pi)^{-1}\int dk\ \tilde{v}_i(z)\exp(ikx+\alpha t), \end{aligned} \tag{13}$$

where k is the wave number, α is the growth rate, and $\tilde{u}_i(z)$ and $\tilde{v}_i(z)$ are the eigenfunctions determined from conservation equations, (3), (4), (7), and (8).

The growth rate of the perturbations to the surface displacement and fluid velocity fields are expressed as an asymptotic expansion in the parameter ϵ. Our subsequent analysis indicates that the first correction to the displacement and velocity fields is $O(\epsilon^{1/2})$, and in anticipation of this we use the following asymptotic expansions for the growth rate and the displacement and velocity fields:

$$\begin{aligned} \alpha&=\alpha^{(0)}+\epsilon^{1/2}\alpha^{(1)}+\cdots,\\ \tilde{u}_i&=\tilde{u}_i^{(0)}+\epsilon^{1/2}\tilde{u}_i^{(1)}+\cdots,\\ \tilde{v}_i&=\tilde{v}_i^{(0)}+\epsilon^{1/2}\tilde{v}_i^{(1)}+\cdots. \end{aligned} \tag{14}$$

The linearized mass and momentum conservation equations [(7) and (8)] for the leading order and $O(\epsilon^{1/2})$ displacement fields are

$$\begin{aligned} &\partial_z\tilde{u}_z^{(0)}+ik\tilde{u}_x^{(0)}=0,\\ &\partial_z\tilde{u}_z^{(1)}+ik\tilde{u}_x^{(1)}=0, \end{aligned} \tag{15}$$

$$-\partial_z\tilde{p}^{(0)}+[-(\alpha^{(0)})^2+\partial_z^2-k^2]\tilde{u}_z^{(0)}=0, \tag{16}$$

$$\begin{aligned} &-\partial_z\tilde{p}^{(1)}-2\alpha^{(0)}\alpha^{(1)}\tilde{u}_z^{(0)}+[-(\alpha^{(0)})^2+\partial_z^2-k^2]\tilde{u}_z^{(1)}=0,\\ &-ik\tilde{p}^{(0)}+[-(\alpha^{(0)})^2+\partial_z^2-k^2]\tilde{u}_x^{(0)}=0, \end{aligned} \tag{17}$$

$$-ik\tilde{p}^{(1)}-2\alpha^{(0)}\alpha^{(1)}\tilde{u}_x^{(0)}+[-(\alpha^{(0)})^2+\partial_z^2-k^2]\tilde{u}_x^{(1)}=0.$$

The expressions for the perturbation to the stresses in the surface are

$$\begin{aligned} &\tilde{\sigma}_{zz}^{(0)}=-\tilde{p}^{(0)}+2\partial_z\tilde{u}_z^{(0)}, \quad \tilde{\sigma}_{xz}^{(0)}=\partial_z\tilde{u}_x^{(0)}+ik\tilde{u}_z^{(0)},\\ &\tilde{\sigma}_{zz}^{(1)}=-\tilde{p}^{(1)}+2\partial_z\tilde{u}_z^{(1)}, \quad \tilde{\sigma}_{xz}^{(1)}=\partial_z\tilde{u}_x^{(1)}+ik\tilde{u}_z^{(1)}. \end{aligned} \tag{18}$$

The eigensolutions for the displacement field are obtained by adding $[-\partial_z\times(17)+ik\times(16)]$, and using Eq. (15) to express $\tilde{u}_x^{(0)}$ and $\tilde{u}_x^{(1)}$ in terms of $\tilde{u}_z^{(0)}$ and $\tilde{u}_z^{(1)}$. The solution contains four eigenfunctions

$$\begin{pmatrix} \tilde{u}_z^{(0)} \\ \tilde{u}_x^{(0)} \\ \tilde{u}_z^{(1)} \\ \tilde{u}_x^{(1)} \end{pmatrix} = \begin{pmatrix} 1 & 1 & 1 & 1 \\ i & (i\lambda/k) & -i & -(i\lambda/k) \\ 0 & (\alpha^{(0)}\alpha^{(1)}z/\lambda) & 0 & (-\alpha^{(0)}\alpha^{(1)}z/\lambda) \\ 0 & i\alpha^{(0)}\alpha^{(1)}(1+\lambda z)/(\lambda k) & 0 & i\alpha^{(0)}\alpha^{(1)}(-1+\lambda z)/(\lambda k) \end{pmatrix} \begin{pmatrix} \exp(kz) \\ \exp(\lambda z) \\ \exp(-kz) \\ \exp(-\lambda z) \end{pmatrix}, \tag{19}$$

where $\lambda = \sqrt{(\alpha^{(0)})^2+k^2}$.

The perturbation to the velocity field in the fluid is described by the linearized Navier–Stokes equations, (3) and (4).

$$\partial_z \tilde{v}_z + ik\tilde{v}_x = 0, \tag{20}$$

$$(\alpha+\Lambda ikz)\tilde{v}_z = -\partial_z\tilde{p} + \epsilon(\partial_z^2-k^2)\tilde{v}_z, \tag{21}$$

$$(\alpha+\Lambda ikz)\tilde{v}_x + \Lambda\tilde{v}_z = -ik\tilde{p} + \epsilon(\partial_z^2-k^2)\tilde{v}_x \tag{22}$$

and the stresses in the fluid are

$$\tilde{\tau}_{zz} = -\tilde{p} + 2\epsilon\partial_z\tilde{v}_z, \quad \tilde{\tau}_{xz} = \epsilon(\partial_z\tilde{v}_x + ik\tilde{v}_z). \tag{23}$$

The characteristic equation for the fluid velocity perturbations is derived by adding $[-\partial_z\times(22)+ik\times(21)]$, and expressing $\tilde{v}_x$ in terms of $\tilde{v}_z$ in the resulting expression using Eq. (20)

$$[-(\alpha+\Lambda ikz)+\epsilon(\partial_z^2-k^2)](\partial_z^2-k^2)\tilde{v}_z = 0. \tag{24}$$

Note that the highest derivative in the above equation is multiplied by the small parameter ϵ, which is a characteristic feature of a singular perturbation problem and indicates the presence of a boundary layer at the interface. Two of the four eigenfunctions of the characteristic equation can be determined by setting $\epsilon=0$ in the characteristic equation. The length scale for the decay of these solutions is $O(H)$, and these solutions are designated the "outer flow solutions," $\tilde{v}_o$. The outer flow solutions are expanded in an asymptotic series in small ϵ

$$\tilde{v}_{oi} = \tilde{v}_{oi}^{(0)} + \epsilon^{1/2}\tilde{v}_{oi}^{(1)} \tag{25}$$

and the characteristic equations for $\tilde{v}_{oz}^{(0)}$ and $\tilde{v}_{oz}^{(1)}$ [from Eq. (24)] are

$$(\alpha^{(0)}+\Lambda ikz)(\partial_z^2-k^2)\tilde{v}_{oz}^{(0)} = 0, \tag{26}$$

$$\alpha^{(1)}(\partial_z^2-k^2)\tilde{v}_{oz}^{(0)} + (\alpha^{(0)}+\Lambda ikz)(\partial_z^2-k^2)\tilde{v}_{oz}^{(1)} = 0. \tag{27}$$

The solution for the characteristic equation (26) is

$$\tilde{v}_{oz}^{(0)} = \exp[-kz], \quad \tilde{v}_{ox}^{(0)} = -i\,\exp[-kz], \tag{28}$$

$$\tilde{p}_o^{(0)} = \left[\frac{\alpha^{(0)}}{k}\exp[-kz] + \frac{i\Lambda}{k}\exp[-kz](1+kz)\right], \tag{29}$$

where the amplitude of the outer flow velocity $\tilde{v}_{zo}^{(0)}$ at the surface has been set equal to 1 without loss of generality. Note that in the above equations, the growing mode proportional to $\exp[kz]$ has been neglected because the velocity fluctuations decay to zero for $z\to\infty$. The characteristic equation for the first correction to the growth rate, $\tilde{v}_{oz}^{(1)}$, Eq. (27), is identical to that for the leading order growth rate $\tilde{v}_{oz}^{(0)}$, Eq. (26), because $(\partial_z^2-k^2)\tilde{v}_{oz}^{(0)}=0$. Therefore, we can set the first correction to the growth rate $\tilde{v}_{oi}^{(1)}=0$ without loss of generality.

The other solutions for the characteristic equation (24) decay within a boundary layer of thickness $O(\epsilon^{1/2}H)$ from the interface, and these are designated the "boundary layer solutions." These are obtained by scaling the z coordinate by $\epsilon^{1/2}H$ in the characteristic equation (24). It turns out that the leading order boundary layer velocity $\tilde{v}_{ix}^{(0)}$, which is obtained from the following equation, is sufficient for the present analysis:

$$[-(\alpha^{(0)}+ik\Lambda z)+\partial_{z'}^2]\tilde{v}_{ix}^{(0)} = 0, \tag{30}$$

where z' is $\epsilon^{-1/2}z$. The solution for the velocity field in the boundary layer is

$$\tilde{v}_{ix}^{(0)} = B_i\,\exp(-\sqrt{\alpha^{(0)}}z'),$$

$$\tilde{v}_{iz}^{(0)} = \frac{ik\epsilon^{1/2}B_i}{\sqrt{\alpha^{(0)}}}\exp(-\sqrt{\alpha^{(0)}}z'), \tag{31}$$

where B_i is determined from the boundary conditions at the interface. Note that $\tilde{v}_{iz}^{(0)}$ is $O(\epsilon^{1/2})$ smaller than $\tilde{v}_{ix}^{(0)}$ in the boundary layer.

At this point, it is instructive to determine the magnitudes of the displacement, velocity, and stress fields. The length scale of flow is the thickness of the surface, H, and the time scale is $(\rho H^2/E)^{1/2}$. If the displacements, $\tilde{u}_z^{(0)}$ and $\tilde{u}_x^{(0)}$, scale as $\tilde{u}$, the scaling of the fluid velocity fields are

$$\tilde{v}_{oz}^{(0)} \sim \left(\frac{E}{\rho H^2}\right)^{1/2}\tilde{u}, \quad \tilde{v}_{ox}^{(0)} \sim \left(\frac{E}{\rho H^2}\right)^{1/2}\tilde{u},$$
$$\tilde{v}_{iz}^{(0)} \sim \epsilon^{1/2}\left(\frac{E}{\rho H^2}\right)^{1/2}\tilde{u}, \quad \tilde{v}_{ix}^{(0)} \sim \left(\frac{E}{\rho H^2}\right)^{1/2}\tilde{u}. \tag{32}$$

The elastic stresses in the surface are $O(E\tilde{u}/H)$, while of magnitudes of the stresses in the outer flow and boundary layer are

$$\tilde{\tau}_{ozz}^{(0)} \sim -\tilde{p}_o + (\epsilon E\tilde{u}/H), \quad \tilde{\tau}_{oxz}^{(0)} \sim (\epsilon E\tilde{u}/H),$$
$$\tilde{\tau}_{izz}^{(0)} \sim (\epsilon E\tilde{u}/H), \quad \tilde{\tau}_{ixz}^{(0)} \sim (\epsilon^{1/2}E\tilde{u}/H). \tag{33}$$

In the above equation, the normal stress, $\tilde{\tau}_{ozz}^{(0)}$ has been separated into the pressure and viscous components, the viscous component of the stress is $O(\epsilon)$ smaller than the pressure. Also note that the shear stress in the inner flow, τ_{ixz}, is $O(\epsilon^{-1/2})$ larger than the normal stress and the viscous stresses in the outer region, which is characteristic of boundary layer flows.

The relative magnitudes of the velocity and stress fields permit us to neglect certain terms in the boundary conditions at the interface, and we are left with the following leading order matching conditions at $z=h(x)$:

$$\alpha^{(0)}\tilde{u}_z^{(0)}=\tilde{v}_{oz}^{(0)}, \quad \alpha^{(0)}\tilde{u}_x^{(0)}=\tilde{v}_{ix}^{(0)}+\tilde{v}_{ox}^{(0)}+\Lambda\tilde{u}_z^{(0)},$$
$$\sigma_{zz}^{(0)}=-\tilde{p}_o^{(0)}, \quad \tilde{\sigma}_{xz}^{(0)}=0. \tag{34}$$

The last term on the right side of the x velocity boundary condition represents the change in the mean velocity at the interface due to an increase in the height of the surface.[3] In deriving this, we have set $h(x)=u_z|_{z=0}$, which is permissible for small displacements. The above boundary conditions permit the following important simplification in the analysis. The matching condition for the velocity in the z direction and the shear and normal stresses in Eq. (34) are independent of the velocity in the boundary layer, and therefore the characteristic equation for the leading order growth rate, $\alpha^{(0)}$, does not depend on the magnitude of the boundary layer velocity. The solutions for the displacement field $\tilde{u}^{(0)}$, Eq. (19), the stress in the surface, Eq. (18), and the outer flow velocity field $\tilde{v}_{oz}$, Eq. (28), and pressure $\tilde{p}_o^{(0)}$, Eq. (29), are substituted into the matching conditions for the z velocity and the stress conditions in Eq. (34), to give the following 5×5 characteristic matrix:

$$\begin{pmatrix} \alpha^{(0)} & \alpha^{(0)} & \alpha^{(0)} & \alpha^{(0)} & 1 \\ (\lambda^2/k)+k & 2\lambda & -(\lambda^2/k)-k & -2\lambda & -(\alpha^{(0)}+i\gamma)/k \\ 2ik & (i\lambda^2/k)+ik & 2ik & (i\lambda^2/k)+ik & 0 \\ \exp(-k) & \exp(-\lambda) & \exp(k) & \exp(\lambda) & 0 \\ i\exp(-k) & (i\lambda/k)\exp(-\lambda) & -i\exp(k) & -(i\lambda/k)\exp(\lambda) & 0 \end{pmatrix}. \tag{35}$$

In the characteristic matrix, the first row arises from the continuity of the velocity in the z direction, the second and third rows are due to the continuity of normal and tangential stress conditions in Eq. (34) while the fourth and fifth rows are a consequence of the zero displacement condition at $z=-1$ Eq. (11). The amplitude for the velocity in the boundary layer, B_i, is determined from the boundary condition for the velocity in the x direction

$$B_i=(-\tilde{v}_x^{(0)}-\Lambda\tilde{u}_z^{(0)}+\alpha^{(0)}\tilde{u}_x^{(0)})|_{z=0}. \tag{36}$$

The characteristic equation for the growth rate, which is the determinant of the characteristic matrix, admits multiple solutions, all of which are imaginary indicating that the perturbations are neutrally stable in the leading order approximation. For $\Lambda=0$, the solutions for the characteristic frequency $\omega=\alpha^{(0)}/i$ are equidistant from the real axis. The magnitude of the characteristic frequency, $|\omega|$, is shown as a function of k for $\Lambda=0$ in Fig. 2. The characteristic frequency assumes values of $(\pm\pi/2)$, $(\pm3\pi/2)$,..., for $k\to0$, and increases proportional to k for large k. The effect of variations in Λ on the lowest harmonic is shown in Figs. 3 and 4; the trend is similar for the higher harmonics. We find that an increase in Λ tends to decrease the frequency of perturbations with positive ω (which represent waves traveling opposite to the direction of flow) and tends to increase the frequency of perturbations with negative ω (which represents waves traveling along the flow direction).

The structure factor for the fluctuations is calculated from the change in the free energy due to the displacement of the interface.[2] The change in the free energy due to the displacement field in the elastic surface is given by

$$F_s=\left(\int dx \int_{-1}^{0} dz[\tfrac{1}{4}(\partial_i u_j+\partial_j u_i)^2+\tfrac{1}{2}(\partial_t u_i)^2]\right), \tag{37}$$

where the free energy has been scaled by (EH^2). The first term in the integral on the right side represents the elastic energy due to the strain in the surface,[14] while the second

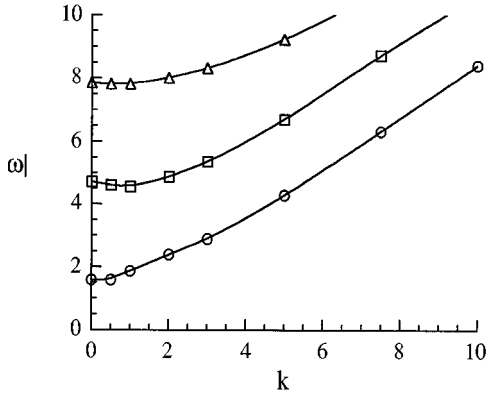

FIG. 2. The first three harmonics of the leading order frequency $|\omega|$ at $\Lambda=0$.

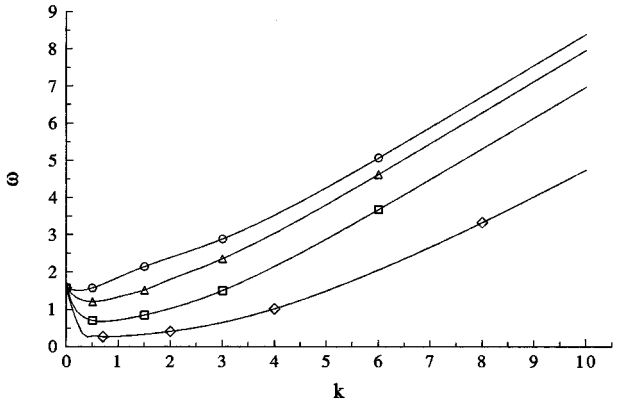

FIG. 3. Effect of variation in Λ on the leading order frequency ω for upstream traveling waves ($\omega>0$). (○) $\Lambda=0$; (△) $\Lambda=3$; (□) $\Lambda=10$; (◇) $\Lambda=30$.

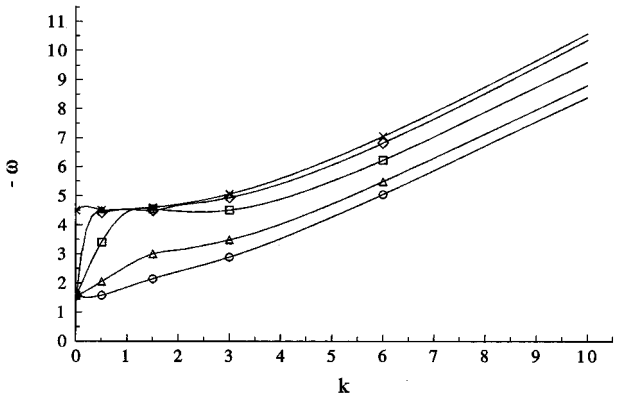

FIG. 4. Effect of variation in Λ on the leading order frequency ω for downstream traveling waves ($\omega<0$). ($\bigcirc$) $\Lambda=0$; ($\triangle$) $\Lambda=3$; ($\square$) $\Lambda=5$; ($\diamond$) $\Lambda=30$; ($\times$) $\Lambda=\infty$.

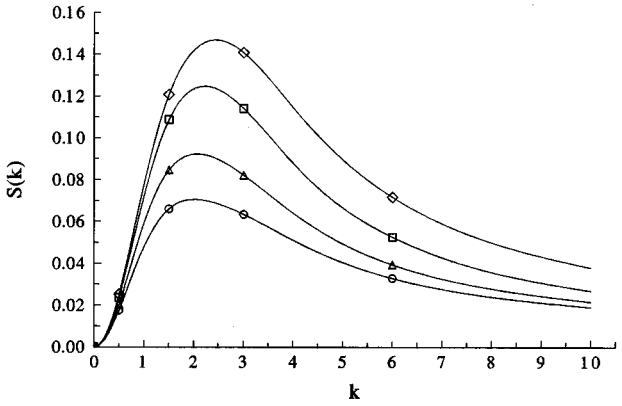

FIG. 5. Effect of variation in Λ on the structure factor for upstream traveling waves. ($\bigcirc$) $\Lambda=0$; ($\triangle$) $\Lambda=3$; ($\square$) $\Lambda=5$; ($\diamond$) $\Lambda=30$.

term is the kinetic energy due to the motion of the elastic medium. The kinetic energy due to the fluid motion above the surface is given by

$$F_f=\left[\int dx \int_0^\infty dz(\tfrac{1}{2}v_i^2)\right]. \tag{38}$$

It is convenient to express the changes in the free energy in terms of the Fourier modes $\tilde{v}_i$ and $\tilde{u}_i$

$$F_s=\int_{\mathbf{k}}\int_{-1}^{0} dz[\partial_z\tilde{u}_z\partial_z\tilde{u}_z^*+k^2\tilde{u}_x\tilde{u}_x^*+(\tfrac{1}{2})(\partial_z\tilde{u}_x+ik\tilde{u}_z) \times(\partial_z\tilde{u}_x^*-ik\tilde{u}_z^*)+\alpha\alpha^*(\tilde{u}_z\tilde{u}_z^*+\tilde{u}_x\tilde{u}_x^*)] \tag{39}$$

$$F_f=\int_{\mathbf{k}}\int_0^\infty dz(\tilde{v}_z\tilde{v}_z^*+\tilde{v}_x\tilde{v}_x^*), \tag{40}$$

where $\int_{\mathbf{k}}$ represents $(2\pi)^{-2}\int d\mathbf{k}$. The change in free energy due to a variation in the height of the interface $\tilde{u}_z(\mathbf{k})$ can be expressed in terms of the structure factor for the correlations of the surface modes[2]

$$F=\tfrac{1}{2}\int_{\mathbf{k}} S(\mathbf{k})^{-1}\tilde{u}_z(\mathbf{k})\tilde{u}_z^*(\mathbf{k}). \tag{41}$$

Equation (41) is similar in form to Eqs. (39) and (40) after the integration over the z coordinate has been carried out. Thus, the structure factor $S(\mathbf{k})$ can be determined by carrying out the integral in Eqs. (39) and (40) over the z coordinate, and expressing the result in terms of $\tilde{u}_z(\mathbf{k})$. The leading order value of $S(k)$, scaled by (EH^2/T), is determined by inserting the leading order growth rate $\alpha^{(0)}$ and the displacement and velocity fields $\tilde{u}_i^{(0)}$ and $\tilde{v}_i^{(0)}$ into Eqs. (39) and (40).

The effect of fluid flow on the leading order structure factor $S(\mathbf{k})$ for waves traveling upstream is shown in Fig. 5. The increase in the structure factor indicates that the amplitude of the upstream waves is amplified, and this can be explained as follows. As the fluid velocity increases, the frequency of the upstream traveling waves decreases (see Fig. 3), and therefore the kinetic energy required for a perturbation of a given amplitude decreases, thereby increasing the amplitude of the fluctuations. The opposite effect is observed for the structure factor of the downstream traveling waves in Fig. 6, because the frequency of these waves increases as the fluid velocity is increased. Further, it can be seen that the structure factor decreases to zero at an intermediate wave number $k=1.23$ for higher fluid velocities, and develops a double-peaked structure. The decrease in $S(k)$ to zero at a finite value of k is because the ratio $(\tilde{u}_x^{(0)}/\tilde{u}_z^{(0)})$ at the interface diverges at this point, and therefore the energy required to produce a change in the height of the interface diverges.

The leading order calculation has proved inconclusive for determining the growth rate of the fluctuations, and it is necessary to determine the $O(\epsilon^{1/2})$ correction to the growth rate, $\alpha^{(1)}$. This calculation is similar to that for $\alpha^{(0)}$, and the details are not given here. The real part of the first correction to the decay rate, $-\mathrm{Re}(\alpha^{(1)})$, is shown as a function of k for the first three harmonics in Fig. 7. The behavior of $-\alpha^{(1)}$ is very different from that of the decay rate for the modes at the interface between a gel and air or vacuum.[2] In that calculation, it was found that the decay rate increases monotonically as the wave number is increased, and the increase is proportional to k^2 for large k. However, in the present case we find that the decay rate increases proportional to $k^{3/2}$ for the lowest harmonic, and *decreases* proportional to $k^{-3/2}$ in the limit $k\gg1$ for the higher harmonics. This is because the energy

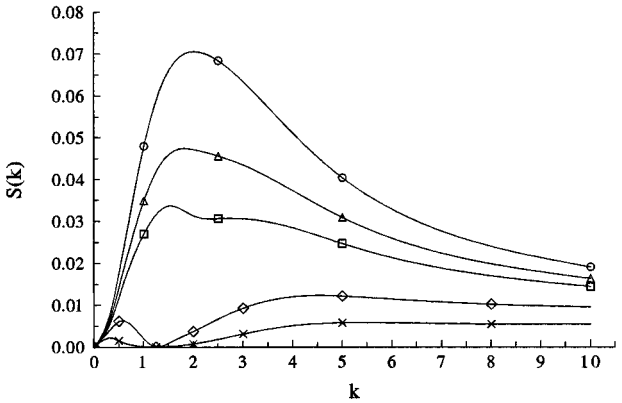

FIG. 6. Effect of variation in Λ on the structure factor for downstream traveling waves. ($\bigcirc$) $\Lambda=0$; ($\triangle$) $\Lambda=3$; ($\square$) $\Lambda=7$; ($\diamond$) $\Lambda=10$; ($\times$) $\Lambda=100$.

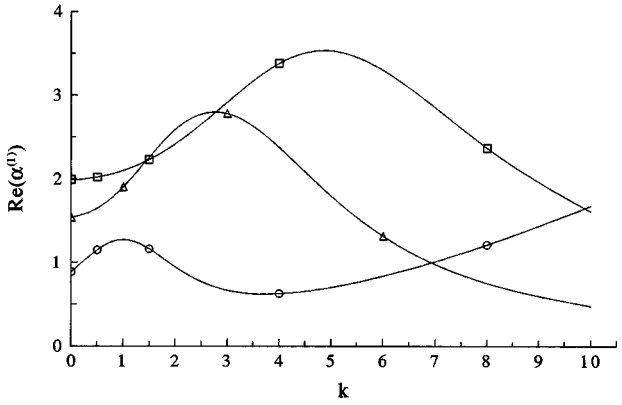

FIG. 7. The $O(\epsilon^{1/2})$ correction to the growth rate $\alpha^{(1)}$. (○) First harmonic; (△) second harmonic; (□) third harmonic.

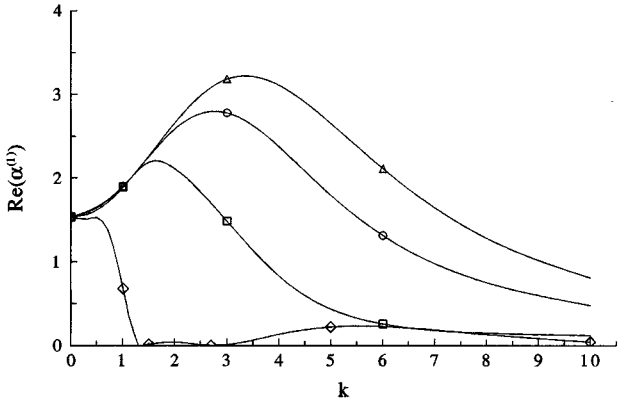

FIG. 9. The effect of variation in Λ on the $O(\epsilon^{1/2})$ correction to the growth rate $\alpha^{(1)}$ for the second harmonic. (○) $\Lambda=0$; (△) $\Lambda=5$ upstream waves; (□) $\Lambda=5$ downstream waves; (◇) $\Lambda=10$ downstream waves.

dissipation in the present case occurs in the boundary layer in the fluid, in contrast to the fluctuations at the gel–air interface where the dissipation takes place in the gel.

The effect of fluid flow on the decay rates of the fluctuations is considered next. Figures 8 and 9 show the real part of $\alpha^{(1)}$ as a function of k for $\Lambda=5$ and $\Lambda=10$ for perturbations with $\omega>0$ (waves traveling upstream). There is an increase in the decay rate as the velocity is increased, due to the increased dissipation in the boundary layer. The behavior of $\mathrm{Re}(\alpha^{(1)})$ for waves traveling downstream $\omega<0$ is shown in Figs. 8 and 9. An increase in the fluid velocity tends to decrease the decay rate, and $\alpha^{(1)}=0$ for certain values of γ, implying that the waves are neutrally stable at these points. The locus of these points in $k-\gamma$ space for the first four harmonics are shown in Fig. 10. Along these lines, the $O(\epsilon^{1/2})$ correction to the growth rate is zero, indicating that the waves are neutrally stable at this level of approximation. This is because the amplitude of the boundary layer velocity, B_i Eq. (36), is identically zero along these points, and therefore there is no dissipation in the boundary layer. To determine the decay rates of the neutrally stable waves, it is necessary to determine the $O(\epsilon)$ correction to the growth rate $\alpha^{(2)}$ along the lines shown in Fig. 10. This is determined in a manner similar to the leading order and $O(\epsilon^{1/2})$ calculations, though it is necessary to include the viscous stresses in the fluid and the elastic medium. We find that $\alpha^{(2)}$ has the form $\alpha^{(2)}=\alpha_1^{(2)}+\eta'\alpha_2^{(2)}$. Figures 10 and 11 show $\alpha_1^{(2)}$ and $\alpha_2^{(2)}$ as a function of k for the parameter values where $\alpha^{(1)}=0$. It is found that both $\alpha_1^{(2)}$ and $\alpha_2^{(2)}$ are negative, indicating that the dissipation in the outer flow and elastic medium have a small stabilizing effect on the fluctuations.

IV. CONCLUSIONS

In this section, the important features of the high Reynolds number flow near an elastic surface are first discussed, and the results of the analysis are compared with the experimental observations of Hansen and Hunston.[4] The system consists of a linear flow of a fluid of infinite extent adjacent to an elastic surface of thickness H. The dynamics of the fluctuations is governed by two dimensionless parameters—the Reynolds number, $\mathrm{Re}=(\rho\gamma H^2/\eta)$, and the dimensionless parameter, $\Lambda=(\rho\gamma^2H^2/E)^{1/2}$, where γ is the strain rate in the fluid, ρ and η are the fluid density and viscosity, and E is the coefficient of elasticity of the surface. The parameter Λ is the ratio of the inertial stresses in the fluid and the elastic

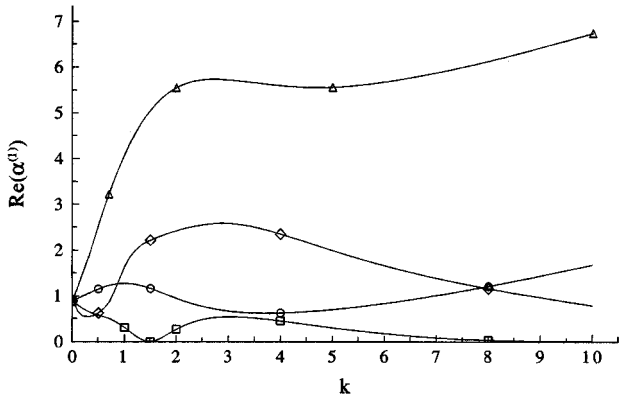

FIG. 8. The effect of variation in Λ on the $O(\epsilon^{1/2})$ correction to the growth rate $\alpha^{(1)}$ for the first harmonic. (○) $\Lambda=0$; (△) $\Lambda=5$ upstream waves; (□) $\Lambda=5$ downstream waves; (◇) $\Lambda=10$ downstream waves.

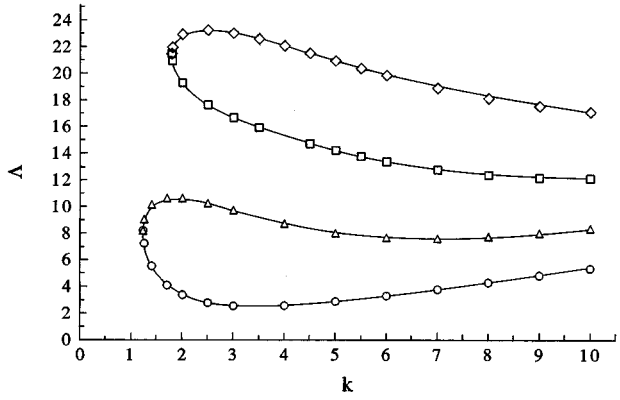

FIG. 10. Lines in $\Lambda-k$ plane where the first correction to the growth rate $\alpha^{(1)}=0$. (○) First harmonic; (△) second harmonic; (□) third harmonic; (◇) fourth harmonic.

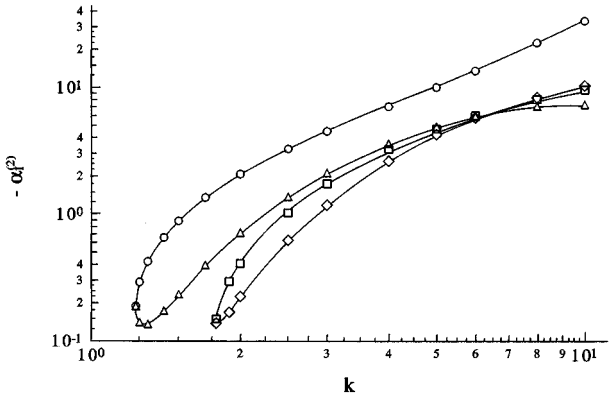

FIG. 11. The second correction to the growth rate, $\alpha_1^{(2)}$, as a function of k for the curves in $\Lambda-k$ space where $\alpha^{(1)}=0$. (○) First harmonic; (△) second harmonic; (□) third harmonic; (◇) fourth harmonic.

stresses in the surface. At high Reynolds number, we used an asymptotic expansion in the small parameter $\epsilon=(\Lambda/\mathrm{Re})$. The leading order flow in the fluid is inviscid, but the viscous stresses are $O(\epsilon^{1/2})$ smaller than the inertial stresses in a boundary layer of thickness $(\epsilon^{1/2}H)$ at the interface. The leading order growth rate, $\alpha^{(0)}$, obtained by solving the inviscid equations of motion, has the same characteristics as the frequency at a gel–air interface.[2] There are multiple frequencies of oscillation, all of which are consistent with the boundary conditions imposed on the elastic surface. In the absence of fluid flow, the frequencies have values of $(\pi/2)$, $(3\pi/2)\cdots$ in the limit $k\to 0$, and increase proportional to k for large k, where k is the wave number of the perturbation.

A shear flow tends to increase the frequency of waves traveling downstream, and decrease the frequency of the waves traveling upstream. The structure factor of the surface waves was calculated from the total energy of the fluctuations, which is the sum of the elastic strain energy in the elastic medium and the kinetic energy in the medium and fluid. The structure factor of the upstream traveling waves is increased by the flow, because the kinetic energy of fluctuations for a given amplitude decreases due to a decrease in the frequency. The opposite effect is observed for waves traveling downstream. In addition, the structure factor has a double-peaked structure and approaches zero at an intermediate wave number, due to the divergence in the ratio of the tangential and normal displacements at this wave number.

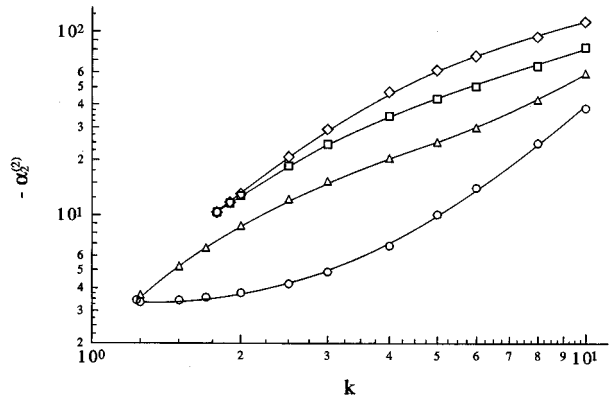

FIG. 12. The second correction to the growth rate, $\alpha_2^{(2)}$, as a function of k for the curves in $\Lambda-k$ space where $\alpha^{(1)}=0$. (○) First harmonic; (△) second harmonic; (□) third harmonic; (◇) fourth harmonic.

The characteristics of the decay rate of the fluctuations is very different from that of a gel–air interface. In the present case, the leading order decay rate is $O(\epsilon^{1/2})$ smaller than the frequency of fluctuations due to the presence of a viscous boundary layer in the fluid, while the decay rate of the surface modes at a gel–air interface is $O(\epsilon)$ smaller than the leading order frequency due to the dissipation in the bulk of the gel. The $O(\epsilon^{1/2})$ correction to the growth rate $\alpha^{(1)}$ was determined by including the effect of the boundary layer velocity. The real part of $\alpha^{(1)}$ is negative for all values of k and Λ, except along certain lines in the $k-\Lambda$ parameter space where it is zero, indicating that the fluctuations are neutrally stable at this order of approximation. Along these lines, the amplitude of the boundary layer velocity becomes zero, and consequently there is no dissipation in the boundary layer. The real part of the $O(\epsilon)$ correction to the growth rate $\alpha^{(2)}$ was found to be negative along these lines, indicating the presence of a small stabilizing effect due to the dissipation in the bulk of the fluid and the elastic medium.

We now compare the results of the analysis with the experimental observations of Hansen and Hunston.[4] Their experimental system consisted of a disk of an elastic material which was spun in a container fluid, and they observed the appearance of waves on the elastic surface when the angular velocity exceeded a critical value. Silberberg[5] analyzed these results in detail, and showed that the waves appear when the critical Reynolds number $(\rho\omega a^2/\eta)$ exceeds $1.2R_G^{1/2}$, where $R_G=(Ea^3\rho/4H\eta^2)$, a is the radius of the disk, and ω is the angular velocity. Note that the parameter R_G is proportional to ϵ^{-2}, since the ratio (a/H) was a constant in the experiments. If we assume that the strain rate at the surface is proportional to the angular velocity, the experimental observations indicate that the fluctuations are unstable when Λ exceeds a critical value. Though the present analysis does not predict an instability, it is found that the first correction to the growth rate $\alpha^{(1)}$ becomes zero for a specific value of Λ, indicating the presence of slowly decaying waves. These may be destabilized by some effect that is not included in this simplified analysis, such as curvature in the velocity profile or nonuniformity in the elasticity of the surface. A comparison of the numerical value of the critical Λ is not possible, however, because we do not have an exact knowledge of the strain rate at the surface of the disk as a function of the angular velocity, and the viscosity of the compliant material.

[1] J. L. Harden, H. Pleiner, and P. A. Pincus, J. Chem. Phys. **94**, 5208 (1991).
[2] V. Kumaran, J. Chem. Phys. **98**, 3429 (1993).
[3] V. Kumaran, G. H. Fredrickson, and P. Pincus, J. Phys. II France **4**, 893 (1994).
[4] R. J. Hansen and D. L. Hunston, J. Sound Vibration **34**, 297 (1974).
[5] A. Silberberg, Physicochem. Hydrodyn. **9**, 419 (1987).
[6] P. Krindel and A. Silberberg, J. Coll. Interface Sci. **71**, 39 (1979).

[7] J. Klein, D. Perahia, and S. Warburg, Nature **143**, 352 (1991).
[8] J. Riley, M. Gad-el-Hak, and R. W. Metcalfe, Ann. Rev. Fluid Mech. **20**, 393 (1988).
[9] T. B. Benjamin, J. Fluid Mech. **6**, 161 (1959).
[10] T. B. Benjamin, J. Fluid Mech. **16**, 436 (1963).
[11] M. T. Landahl, J. Fluid Mech. **13**, 609 (1962).
[12] P. W. Carpenter and A. D. Garrad, J. Fluid Mech. **155**, 464 (1985).
[13] P. W. Carpenter and A. D. Garrad, J. Fluid Mech. **170**, 199 (1986).
[14] L. D. Landau and E. M. Lifshitz, *Theory of Elasticity* (Pergamon, New York, 1989).